

# Structural Heart

## The Journal of the Heart Team

ISSN: 2474-8706 (Print) 2474-8714 (Online) Journal homepage: <https://www.tandfonline.com/loi/ushj20>

## 3D Hybrid Imaging for Structural and Congenital Heart Interventions in the Cath Lab

Hans Thijs van den Broek, René van Es, Gregor J. Krings, Quirina M. B. De Ruiter, Michiel Voskuil, Mathias Meine, Peter Loh, Pieter A. Doevendans, Steven A. J. Chamuleau & Frebus J. van Slochteren

To cite this article: Hans Thijs van den Broek, René van Es, Gregor J. Krings, Quirina M. B. De Ruiter, Michiel Voskuil, Mathias Meine, Peter Loh, Pieter A. Doevendans, Steven A. J. Chamuleau & Frebus J. van Slochteren (2018) 3D Hybrid Imaging for Structural and Congenital Heart Interventions in the Cath Lab, *Structural Heart*, 2:5, 362-371, DOI: [10.1080/24748706.2018.1490841](https://doi.org/10.1080/24748706.2018.1490841)

To link to this article: <https://doi.org/10.1080/24748706.2018.1490841>



© 2018 The Author(s). Published by Taylor & Francis.



Published online: 19 Jul 2018.



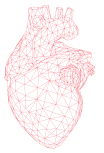
Submit your article to this journal [↗](#)




Article views: 583



View Crossmark data [↗](#)



## 3D Hybrid Imaging for Structural and Congenital Heart Interventions in the Cath Lab

Hans Thijs van den Broek, MSc <sup>a</sup>, René van Es, PhD<sup>a</sup>, Gregor J. Krings, MD, PhD<sup>c</sup>, Quirina M. B. De Ruiter, PhD<sup>b</sup>, Michiel Voskuil, MD, PhD<sup>a</sup>, Mathias Meine, MD, PhD<sup>a</sup>, Peter Loh, MD, PhD<sup>a</sup>, Pieter A. Doevendans, MD, PhD<sup>a,d</sup>, Steven A. J. Chamuleau, MD, PhD<sup>a</sup>, and Frebus J. van Slochteren, PhD<sup>a</sup>

<sup>a</sup>Department of Cardiology, University Medical Center Utrecht, Utrecht, The Netherlands; <sup>b</sup>Department of Vascular Surgery, University Medical Center Utrecht, Utrecht, The Netherlands; <sup>c</sup>Department of Paediatric Cardiology, Wilhelmina Children's Hospital, University Medical Center Utrecht, Utrecht, The Netherlands; <sup>d</sup>Netherlands Heart Institute, Utrecht, The Netherlands

### ABSTRACT

Hybrid imaging (HI) during cardiovascular interventions enables the peri-procedural visualization of the organs and tissues by means of integrating different imaging modalities. HI can improve the procedural efficacy and safety. This review provides an overview of different systems, their possibilities and the current clinical use and benefits focused on structural and congenital heart diseases. We have performed a literature search and linked the software options to the clinical use in cardiology to gain insight into the clinical use of the systems. In this review, we focus on radiation and contrast exposure, complication rate and procedure time. We found that currently available studies are limited by small cohorts. Nevertheless, HI systems for valvular procedures result in a significant decrease of radiation and contrast exposure. The largest benefit hereof is observed when HI is used in combination with rotational angiography. Furthermore, automatically determined optimal implant angle for transcatheter aortic valve implantation decreases the complication rate significantly. Congenital heart disease interventions that require 2D/3D Transoesophageal echocardiography (TEE) such as septal defects show a significant decrease in radiation and contrast exposure and procedural time when using TEE-Mono- and bi-plane cine angiography and fluoroscopy (XRF) fusion software. MitraClip procedures using these HI systems, however, show only a trend in decrease of these effects. In conclusion, major interventional X-ray vendors offer HI software solutions which are safe and can aid the planning and image guidance of cardiovascular interventions. Even though current HI technologies have limitations, HI provides support in the increasingly complex cardiac interventional procedures to provide better patient care.

**ARTICLE HISTORY** Received 17 January 2018; Revised 17 May 2018; Accepted 14 June 2018

**KEYWORDS** 3D rotational angiography; cone-beam computed tomography; hybrid imaging; image-guided interventions; image fusion; 3D guidance

### Introduction

Structural heart disease (SHD) and congenital heart disease (CHD) interventions involve a wide range of procedures which have expanded significantly during the last years. Minimal invasive therapies such as transcatheter aortic valve implantation (TAVI), devices for atrial septal defects (ASD), or clips to treat mitral regurgitation have become alternatives for surgical procedures.<sup>1–4</sup> As the expanding portfolio of interventional cardiology comes with new challenges, a need for imaging tools to support the cardiologist has arisen.

Standard mono- and biplane X-ray cine angiography and fluoroscopy (XRF) used during interventional cardiology procedures, primarily enable contrast-based visualization and are less suitable for the characterization of soft tissues. The increasing complexity of interventional procedures requires visualization of the topographic surrounding of interventional targets. This increases the radiation exposure and use of contrast medium during these interventions, which is potentially harmful to the patients and staff.<sup>5</sup> This paradigm drives the development of new techniques aiming to improve visualization while reducing radiation and contrast exposure. Currently, XRF is often supported side-by-side by pre- or peri-procedurally acquired

imaging modalities as 2D/3D ultrasound, MRI, CT or a combination of these. Fusion of multiple imaging modalities, for instance fluoroscopy with CT, is referred to as hybrid imaging (HI).<sup>6</sup>

HI during cardiovascular interventions enables the peri-procedural visualization of the organs and tissues acquired by means of integrating different imaging modalities. HI can improve the procedural efficacy and safety. This review provides an overview of different hybrid fusion imaging technologies incorporating rotational angiography, their possibilities and the current clinical use and benefits for structural and congenital heart diseases.

### Materials and methods

We performed a PubMed and Embase search to identify full-text reports describing the use of image-guided structural, valvular and cardiac device closure interventions. In addition to the search results, we searched the references of relevant articles retrieved by the search strategy. Search terms included cardiac, structural heart disease or congenital heart disease; and image guidance, image guided, image-guided therapy, hybrid

imaging, fusion imaging or 3D imaging. Hereafter we linked the software options to the clinical application to gain insight into the use of the systems (e.g. radiation exposure, procedural time, complication rate etc.). Additionally, we have contacted the four largest interventional XRF companies (Philips Healthcare, Siemens Healthineers, GE Healthcare, and Canon Medical) and collected all necessary data to provide an overview of the different systems and their possibilities.

This article will briefly discuss the imaging modalities used for HI and review various types of interventions using HI divided into SHD (i.e. valvular interventions) and CHD (i.e. septal defects and obstructive lesions).

## Imaging modalities used in HI

### Pre-procedurally acquired imaging

The most frequently used pre-procedural imaging modalities that are integrated with live XRF images are Ultrasound and CT. However, cardiac MRI is increasingly used in the diagnostic workup in cardiovascular diseases and allows assessment of the function and structure of the cardiovascular system (e.g. heart function, myocardial infarct visualization, and perfusion imaging),<sup>7</sup> use of CMR for hybrid imaging (HI) is still limited.

Cardiac CT is routinely used to evaluate coronary heart disease, evaluate heart and valve function, and assess calcium build-up in the coronary arteries and aorta. Modern CT setups use a multi-detector technique (up to 320 detectors). The high number of detectors results in high resolution 3D cardiac imaging data.<sup>1</sup>

### Peri-procedurally acquired imaging

Traditionally, transoesophageal echocardiography (TEE) has been an important aid alongside XRF in structural and congenital heart procedures to facilitate amongst others, transcatheter mitral valve repair, trans-septal punctures (TSP), and closure of septal defects or paravalvular leaks.<sup>8</sup> TEE provides sufficient visualization of soft tissue whereas 3D TEE facilitates realistic representation of cardiac structures and allows navigation in 3D space. However, interpreting the images of

TEE alongside XRF is difficult due to the different image orientation of the two modalities.

Cone-beam CT (CBCT), also referred to as C-arm CT, allows physicians to obtain a 3D volume reconstruction during the interventional procedure, from a single gantry rotation of a flat-panel detector XRF imaging setup.<sup>9</sup> The 3D volume obtained with CBCT resolves low contrast objects. CBCT is the underlying mechanism of a 3D rotational angiography (3DRA), which incorporates a contrast injection during the gantry rotation to visualize highly contrast enriched objects. The latter technique requires contrast injection in the proximal cavity of the region of interest during the entire rotation, to visualize the tissue-blood border, the depot effect. During the procedure, a 3D anatomical roadmap, acquired with 3DRA, can be superimposed onto the live XRF images (Figure 1). This provides e.g. instant visualization of the large arteries and the interventional devices. Furthermore, CBCT-based 3D datasets can also be used to perform 3D to 3D data registration with e.g. CT, MRI, and SPECT (Tables 1 and 2).

### Caution while using HI (radiation and contrast exposure)

CBCT-based HI interventions potentially expose the patient to increased levels of radiation and contrast compared to conventional XRF guidance. The reported radiation and contrast levels for CBCT are significantly lower than the median radiation exposure used in adult cardiac CT, especially with optimized CBCT protocols.<sup>10–15</sup> When used only for anatomical guidance during HI, CBCT is therefore the preferred modality. Moreover, a beneficial effect of CBCT + XRF-based interventions compared to XRF interventions alone on skin dose is seen in patients.<sup>16</sup> The focus for optimizing CBCT protocols for adult patients is on reducing contrast use to limit the kidney burden while in the pediatric patients the focus is on reducing the radiation exposure.<sup>17</sup>

Radiation reduction can be achieved by reducing the collimation, detector entrance dose, and frame rate with preservation of image quality (Table 3).<sup>12,14,18</sup> Several studies have shown that standardized acquisition and contrast protocols have a beneficial effect on radiation exposure and contrast use during SHD (Table 3).<sup>10–13</sup> Siemens systems require a short

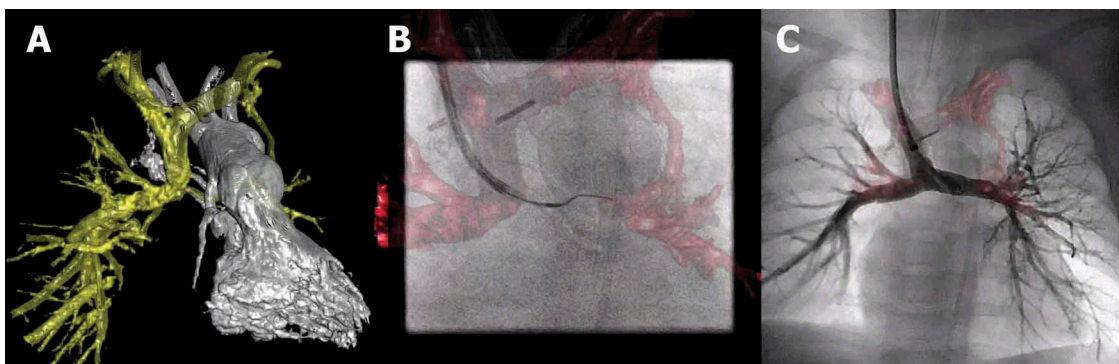


**Figure 1.** Hybrid imaging during recanalization of a partial cavo-pulmonary connection of the left pulmonary artery. (A) 3D reconstruction of the pulmonary artery tree (yellow structure) and left ventricle (LV) with outflow tract (white structure). (B) 3D overlay of the pulmonary tree is used to introduce a guidewire into the left pulmonary artery. (C) Contrast injection in the pulmonary artery tree with the stent in place.

**Table 1.** Overview of advanced imaging options of major XRF vendors.

|                         | Philips Healthcare   |  | Siemens Healthineers  |  | GE Healthcare  |  | Canon Medical   |  |
|-------------------------|--|--|---|--|--|--|---|--|
| Systems                 | Allura Xper FD10/10<br>Allura Xper FD20/10<br>Allura Xper FD20<br>Azurion 5<br>Azurion 7 |  | Artis Q<br>Artis Q.zen<br>Artis zee<br>Artis zeego<br>Artis pheno |  | IGS 3 × 0 <sup>a</sup><br>IGS 5 × 0 <sup>a</sup><br>IGS 6 × 0 <sup>a</sup><br>IGS 7 × 0 <sup>a</sup> |  | Infinix-i systems   |  |
| 3D technology           | 3D Rotational angiography  | Cone-beam CT   | 3D Rotational angiography   | Cone-beam CT                                   | 3D Rotational angiography  | Cone-beam CT   | 3D Rotational angiography   | Cone-beam CT   |
| Products                | 3DRA   | XperCT   | InSpace 3D  | DynaCT   | Innova 3D  | Innova CT HD   | 3D-DA/3D-DSA  | Low contrast imaging   |
| Anatomy best visualized | Contrast filled  | Soft tissue, bones and contrast filled tissues   | Contrast filled   | Soft tissue, bones and contrast filled tissues | Contrast filled  | Soft tissue, bones and contrast filled tissues   | Contrast filled   | Soft tissue, bones and contrast filled tissues   |
| Acquisition time        | 80°/s (240 frames in 4 s)  | 80°/s (120 frames in 4 s)<br>80°/s (240 frames in 4 s)<br>24°/s (300 frames in 10 s)<br>24°/s (620 frames in 10 s) | 40°/s (133 frames in 5 s) <sup>b</sup>                            | 40°/s (248 frames in 5 s) <sup>b</sup>         | 40°/s (approx. 150 frames in 5 s)  | 40°/s (approx. 250 frames in 5 s)<br>28°/s (approx. 350 frames in 7 s)<br>16°/s (approx. 600 frames in 12 s) | 80°/s (250 frames in 2.6 s)<br>80°/s (400 frames in 2.6 s)<br>80°/s (600 frames in 2.6 s) | 25°/s (250 frames in 10 s)<br>26.7°/s (400 frames in 15 s)<br>30°/s (600 frames in 20 s) |
| Angular rotation (°)    | 240  | 240  | 200<br>2×220/360 <sup>c</sup>                                     | 200<br>2×220/360 <sup>c</sup>                  | 200  | 200  | 210   | 210  |
| Frame rate (fps)        | 30   | 30–60  | 26.6 <sup>d</sup>   | 49.6 <sup>d</sup>                              | 30   | 50   | 100 <sup>d</sup>  | 25–30 <sup>d</sup>   |
| Processing time         | 5 seconds (256 <sup>3</sup> )  | < 1min   | < 20s   | < 20s  | < 30s  | < 1min   |   |  |
| Spatial Resolution      | 256 <sup>3</sup>   | 256 <sup>3</sup>   | 256 <sup>3</sup> (512 <sup>3</sup> )                              | 256 <sup>3</sup> (512 <sup>3</sup> )           | 512 <sup>3</sup>   | 512 <sup>3</sup>   | 256 <sup>3</sup> (512 <sup>3</sup> )  | 256 <sup>3</sup> (512 <sup>3</sup> )   |
| Image integration       | CT<br>MR   |  | CT<br>MR<br>PET-CT  |  | CT<br>MR<br>PET-CT<br>SPECT  |  | CT<br>MR  |  |

Notes. <sup>a</sup>X: 2 = 20×20 detector, 3 = 30×30 detector, 4 = 40×40 detector.

<sup>b</sup>Artis Pheno can perform all 3D imaging acquisitions in 4s.

<sup>c</sup>Artis Pheno can perform 360 degrees rotation.

<sup>d</sup>Estimated based on acquisition time and angular rotation.

3DRA, 3D rotational angiography; CBCT, cone-beam CT; CT, computed tomography; MR, magnetic resonance; PET, positron emission tomography; SPECT, single positron emission CT.

image acquisition to be done before starting the DynaCT to calibrate the CBCT settings. Too short image acquisition may result in high tube currents and therefore an unnecessary increase in radiation dose.<sup>12</sup> Next to lowering radiation exposure, the reduced amounts of contrast medium are also beneficial for the safety of the patients.<sup>19</sup>

Important for an adequate 3DRA acquisition is homogeneous contrast density at the entire region of interest during the entire rotation. This requires a contrast protocol to enhance the spatial and temporal resolution of 3DRA. Critical for the contrast administration is the contrast location (depot), the amount of contrast (dilution) and timing of prefilling. In addition, the washout of contrast can be delayed using e.g. rapid ventricular pacing, inducing at least an arterial blood pressure reduction of 50%. Thus enhancing contrast density and edge sharpness. On the contrary, rapid ventricular pacing results in ventricular dimensions which do not represent normal physiological dimensions but are sized between diastolic and systolic dimensions. Furthermore, a breath hold or a respiratory stop during the acquisition minimizes movement of thoracic structures. The respiratory state is also important during registration of MRI or CT datasets. Registration of datasets with

corresponding respiratory states results in a higher registration accuracy.

## Types of interventions using HI

### Valvular interventions

#### Challenges in valvular interventions

Percutaneous valvular interventions are challenging due to: (1) prosthesis selection based on accurate measurement of the valve annulus and the out- or inflow tract, which is critical to prevent paravalvular leakage, coronary occlusion, and possibly cardiac arrhythmias;<sup>20</sup> (2) difficult catheter manipulations with limited manual maneuverability;<sup>21</sup> and (3) limited intraoperative ability to expand the view from 2D to 3D cardiac anatomy including critical anatomical landmarks, e.g. possibly causing occlusion of adjacent coronary arteries.

#### Solutions for aortic valve interventions

To overcome the aforementioned issues for TAVI procedures, all major XRF vendors offer commercial TAVI planning software packages (Table 2). These software packages can automatically delineate the aortic root in CT or CBCT images and

**Table 2.** Overview of HI software tools of major XRF vendors for structural and congenital heart diseases.

| Tools                    | Philips Healthcare   |   | Siemens Healthineers   |   | GE Healthcare   |
|--------------------------|--|---|--|---|---|
|                          | HeartNavigator   | EchoNavigator   | Aortic Valve Guide   | TrueFusion  | HeartVision 2   |
| Image integration        | CT   | Echo (Philips CX50 or iE33, or Philips EPIC)  | CBCT, CT   | Echo (Acuson SC2000 Prime only)   | CBCT, CT, MR, SPECT, PET  |
| Image fusion             | 2D/3D matching of 3D volume with 2D XRF  | Automatic fusion of 3D TEE with 2D XRF  | 2D/3D (2 2D XRF images > 30° apart)  | Automatic fusion of 3D TEE with 2D XRF  | 2D/3D match with 2 orthogonal (AP, Lateral) 2D XRF shots<br>3D/3D match with 3D XRF   |
| Image processing         | 3D/3D match with 3D XRF  | Automatic segmentation: - Left ventricle - Aortic valve - Aorta - Coronary ostia                                      | Automatic segmentation: - Aortic root - Coronary ostia - Aortic valve cusps<br><br>Demarcation of landmarks  | Demarcation of anatomical structures on echo  | Automatic segmentation: - Left cavities (CT) - Left atrium (Innova 3D/CT HD) - Large structures (CT/Innova 3D/Innova CT HD) |
| Measurements             | Automatic: Annulus: - Diameter - Perimeter - Area<br>Aortic: - Diameters above annulus - Ostia heights - Sinus diameters |   | Annulus: - Diameter - Perimeter - Area   | Automatic: Annulus: - Diameter - Perimeter - Area<br>Aortic: - Root Sinotubular junction - Root Sinus of Valsalva     | Automatic: Annulus: - Diameter - Perimeter - Area<br>Aortic: - Diameters above annulus - Ostia heights - Sinus diameters    |
| Roadmap + extra markers  | Real-time 3D volume or outline overlay   | Real-time 3D TEE overlay<br><br>Demarcation of landmarks  | Real-time 3D volume or outline overlay<br>Demarcations of Cusp nadirs, coronary ostia markers and ascending aorta centreline<br><br>Add circle of perpendicularity | Real-time 3D TEE overlay<br><br>Demarcation of landmarks  | Real-time 3D volume overlay<br>Add landmark points and planning lines   |
| Optimal X-ray angulation | Yes<br>TAVI  |   | Yes  | Yes   | Yes<br>TAVI   |
| Additional               | Device selection and view planning<br><br>Calcification distribution ascending aorta                                     | Automatic tracking of TEE transducer position and orientation<br><br>Automatic TEE field of view outline is displayed |  | Automatic tracking of TEE transducer position and orientation<br><br>Automatic TEE field of view outline is displayed |   |

Note. 3DRA, 3D rotational angiography; CBCT, cone-beam CT; CT, computed tomography; MR, magnetic resonance; PET, positron emission tomography; SPECT, single positron emission CT; TAVI, transcatheter aortic valve implantation; TEE, transoesophageal echocardiography; XRF, single- and bi-plane cine angiography and fluoroscopy.

calculate the aortic valve deployment angles based on the position and orientation of the aortic valve annulus.<sup>22</sup> Markers of the aortic root, left and right coronary ostia are automatically superimposed on the live XRF images, thus facilitating intuitive navigation and maneuvering (Figure 2).<sup>22</sup> Furthermore, accurate deployment angles are provided for aortic valve placement.

#### Different implementations for aortic valve interventions

Aortic Valve Guide software (Siemens Healthineers) has shown to reliably fulfill the functionality and significantly reduce procedure time, radiation exposure and use of contrast using CBCT.<sup>22–25</sup> Consequently, a reduction in peri- and post-interventional complications such as device malpositioning, paravalvular leakage, trauma of surrounding structures as well as other organ damage (acute kidney failure) was shown.<sup>22,24</sup> Excellent implant angles determined by Aortic Valve Guide are significantly more likely to be associated

with no paravalvular regurgitation compared to satisfactory or poor implant angles (41.3% vs. 21.6%, respectively,  $p = 0.045$ ) independent of operator experience.<sup>22</sup>

HeartNavigator software (Philips Healthcare) has also shown to provide accurate prosthesis selection, comparable to gold standard CT assessment.<sup>26</sup> In addition, Philips' HeartNavigator has shown to provide accurate planning and guidance to obtain transapical access for, amongst others, paravalvular leakage repair. However, no significant differences in procedural data, contrast and fluoroscopy time were shown compared to obtaining transapical access without HeartNavigator. Although a trend can be seen in reduced contrast volume and XRF time during procedures where HeartNavigator was used.<sup>27</sup>

The use of HeartVision (GE Healthcare) is well described for endovascular aortic repair but there is no literature available that describes the use in cardiac procedures. From the

**Table 3.** Overview of optimized CBCT scan and contrast infusion protocols used for structural and congenital heart disease interventions.

| Source                                   | Adult                        |                             | Pediatric                   |   |
|--|------------------------------|-----------------------------|-----------------------------|---|
|  | Numburi et al. <sup>10</sup> | Balzer et al. <sup>11</sup> | Peters et al. <sup>12</sup> | Haddad et al. <sup>13</sup>                   |
| XRF system                               | Siemens Axiom Artis          | Philips Allura FD20         | Siemens Artis zee           | Toshiba Infinix-I                             |
| Scan duration (s)                        | 5                            | 5.2                         | 5                           | 4.1   |
| Frame rate (frames/s)                    | 60                           | 60                          | 30                          | 25  |
| Angular rotation(°)                      | 220                          | 210                         | 200                         | 206   |
| Number of Projections (frames/scan)      | 235                          | 312                         | 248                         | -   |
| Tube potential (kV)                      | Automatic (75–125)           | 120                         | Automatic                   | 88 (< 30 kg) & 95 (> 30 kg)                   |
| Tube current (mAs)                       | Automatic (150–692)          | Automatic (50–325)          | Automatic (mean 118.4 ±104) | Automatic (25–55)                             |
| Detector entrance dose (μGy/X-ray pulse) | 0.54                         | -                           | -                           | ~0.13–0.22                                    |
| Contrast infusion site                   | Aortic root                  | Left ventricle              | Varying                     | Varying                                       |
| Iodine concentration (mgI/mL)            | 370                          | 350                         | 300                         | -   |
| Total volume (mL/kg) (contrast:saline)   | (~1:1)                       | 0.8 mL/kg (1:1)             | (3:4)                       | 1.6 mL/kg (1:2 for < 30 kg & 2:3 for > 30 kg) |
| Flow rate (mL/s)                         | 10–15                        | 14                          | 2–14                        | -   |
| Injection duration (s)                   | 6–8                          | 6                           | 6                           | 5–6   |
| Scan delay (s)                           | 1–2                          | 1                           | 1                           | 1–2   |
| Gating                                   | Ungated                      | Ungated                     | Ungated                     | Ungated                                       |
| Cardiac rhythm during imaging            | RVP (200 bpm)                | RVP (200 bpm)               | RVP (180+ bpm)              | RVP (140–180 bpm)                             |

Note. The protocols are divided in adult and pediatric protocols, respectively focused on TAVI procedures and reducing radiation and contrast levels while maintaining good image quality. Bpm, beats per minute; RVP, rapid ventricular pacing; XRF, single- and bi-plane cine angiography and fluoroscopy.

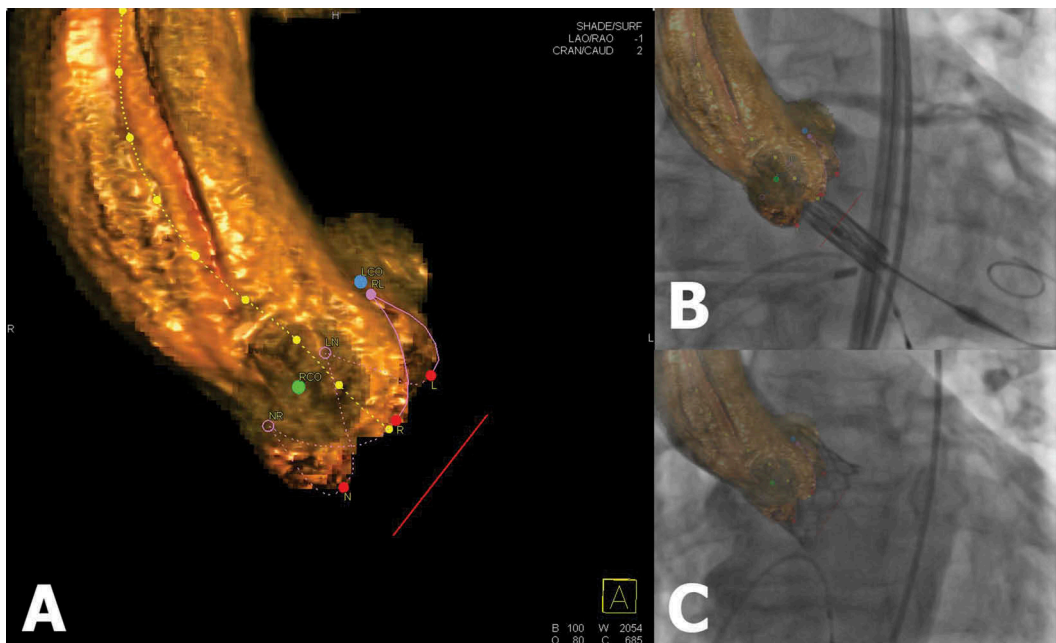


**Figure 2.** Hybrid imaging during TAVI. (A) 3D reconstructed DynaCT of the aortic root using Aortic Valve Guide (Siemens Healthineers) shows automatically generated aortic centerline (marked yellow dotted line), a circle of perpendicularity (marked red line), and coronary ostia markers (blue and green markers). (B, C) The cusps markers (red dots) and circle of perpendicularity enable accurate prosthesis deployment at the correct annular height.

specifications and intended use, it can be deduced that the functionality of the systems of Siemens and GE Healthcare add a wider range of image integration options compared to HeartNavigator (Philips Healthcare) (Table 2). The latter system only allow integration of CT.

### Solutions for mitral valve interventions

Transcatheter mitral valve implantation interventions face similar challenges to TAVI procedures,<sup>28</sup> specific software

solutions, however, are lacking. Mitral valve repair by means of MitraClip device (Abbot Vascular, Santa Clara, CA, USA) procedures are performed under XRF guidance and supported by 2D/3D TEE, which are presented in parallel to most often two cardiologists performing the procedure. TEE-XRF fusion optimizes image representation to allow for a fast and clear understanding of the images when TEE and XRF are used in conjunction.

### Different implementations for mitral valve interventions

Both Siemens and Philips offer software solutions to integrate live 3D TEE with live XRF (Table 2).<sup>8,29</sup> The TEE transducer is automatically tracked in the live XRF images and the 3D echocardiographic images are fused with the XRF images. Demarcations of important soft tissue structures made in the echo images are shown on the live images. Thus allowing accurate assessment for the position of TSP.<sup>30,31</sup> Philips' EchoNavigator guided MitraClip procedures versus conventional TEE-XRF guided MitraClip procedures showed no differences in procedure time and radiation exposure, although a trend towards shorter procedure time was observed.<sup>29,30</sup> Interestingly, EchoNavigator allowed faster placement of two or more clips decreasing the time until the second or third clip by 6 min ( $83.2 \pm 27.4$  vs.  $88.9 \pm 29.0$  min,  $p = 0.6$ ) and 60 min ( $134.2 \pm 23.2$  vs.  $199.5 \pm 72.8$  min,  $p = 0.4$ ) minutes, respectively.<sup>30</sup>

There is no literature on the use of Siemens' TrueFusion TEE-XRF fusion software in cardiac procedures. From the specifications and intended use, it can be deduced that the functionality of TrueFusion is comparable to EchoNavigator. Both TrueFusion and EchoNavigator require specific echo systems to ensure accurate TEE-XRF fusion imaging (Table 2).

### Solutions for other heart valves

For the use of HI in the repair/implantation of the other heart valves the available literature is limited. Pre-procedural image fusion during pulmonary valve implantations using VesselNavigator (Philips Healthcare) has shown to significantly reduce the procedure time, radiation exposure, and contrast levels compared to 2D XRF and 3DRA alone.<sup>32</sup> Another study showed no significant difference of radiation exposure with 3DRA guidance compared to 2D XRF, although a trend of decreased radiation exposure could be seen.<sup>33</sup>

### CHD interventions

#### Challenges in septal defect closures

Septal defect closure with devices are challenging procedures due to: (1) varying morphology of the septal defect, and (2)

the number of defects; (3) prosthesis selection is based on accurate measurement of the septal defect(s).

#### Solutions for septal defect closures

Percutaneous closure of atrial septal defects has shown to benefit from TEE-XRF fusion by EchoNavigator,<sup>34</sup> the integrated information from TEE enabled catheter and device placement at exactly the intended anatomic location in 81% ( $n = 21$ ) of the procedures.<sup>29</sup> Furthermore, TEE-XRF significantly decreased both fluoroscopy time and radiation dose. Besides septal defect closures, TSP is a procedural step in e.g. MitraClip placement and left atrial appendage occlusions. EchoNavigator has shown to be a safe method to guide TSP and significantly decreases the duration to perform TSP ( $18.48 \pm 5.62$  vs.  $23.20 \pm 9.61$  min,  $p = 0.006$ ).<sup>35</sup>

#### Challenges in obstructive lesions

Obstructive lesions such as coarctation of the aorta (CoA) or pulmonary vein stenosis are increasingly treated using a minimally invasive approach. Important for a successful intervention is: (1) accurate 3D imaging of the topographic cardiac surrounding to accurately size the stenosis, and (2) avoid occlusion of adjacent vasculature, e.g. carotid or subclavian arteries.

#### Solutions for obstructive lesions

To overcome these challenges for CoA, integrating 3DRA in the workflow provides important anatomical information and therefore a better understanding of the aortic arch and CoA morphology compared to conventional XRF (Figures 1 and 3).<sup>36</sup> Live XRF overlay of the 3D-reconstructed image allows detailed 3D image guidance without a significant increase in procedural duration or radiation exposure.<sup>37,38</sup> Moreover, pre-procedural imaging can be used for co-registration with XRF and used as roadmaps for live XRF guidance with low registration errors < 4 mm (75%, 21/28 patients).<sup>39,40</sup>

### Discussion

Advanced imaging techniques using HI in clinical use is still in its infancy and far from standard in most Cath labs. Current technologies are limited to planning and visualization of

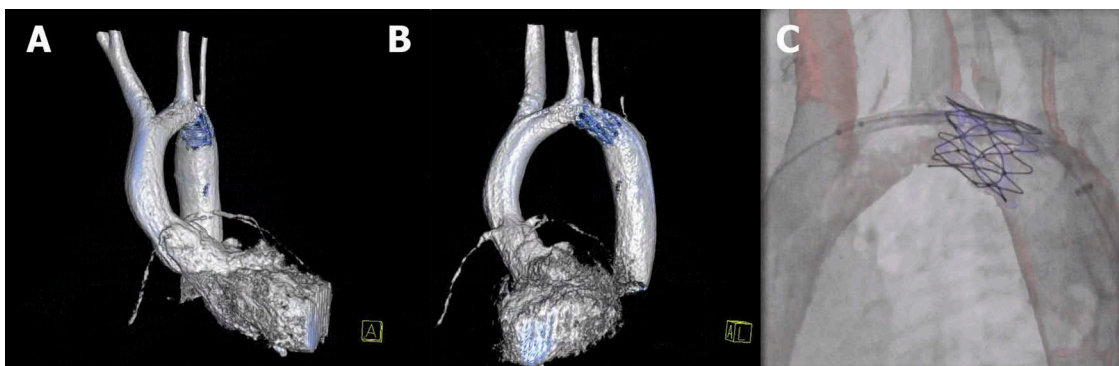


**Figure 3.** Hybrid imaging during stent placement in a coarctation of the aorta. (A,B) 3D reconstruction of the left ventricle and aorta (white structure) and stent in the aortic arch (blue structure), respectively shown in the AP and LAO projections. (C) 3D overlay of the aortic arch with the stent in place. The 3D roadmap is used to provide targeted stent placement and avoid obstruction of the left common carotid and left subclavian arteries.



anatomy only. The studies included in our review are focused on the impact of hybrid fusion imaging technology on the short-term outcome compared to the multi-modality approach. Available tools have shown a significant decrease in fluoroscopy time, radiation dose, contrast medium use, and in some cases a shorter procedure time is achieved. These procedural outcomes can be directly attributed to the use of hybrid fusion technology. In daily practice, HI solutions can be integrated smoothly into the workflow in the catheterization lab, providing important visualization of 3D cardiac anatomy and surrounding organs. Most studies report on the use of Siemens' Aortic Valve Guide or Philips' EchoNavigator.

Fusion of CBCT or 3DRA with XRF is currently most used for guidance of TAVI's in combination with Siemens' Aortic Valve Guide. The advantage of using CBCT techniques over pre-procedural imaging are the maintained patient position, volume status and physiology between the time of imaging and intervention.<sup>41</sup> Furthermore, compared to pre-procedural CT, the radiation and contrast exposure of CBCT is significantly lower.<sup>11,22</sup>

TEE-XRF fusion is increasingly used in mitral valve repair and various CHD procedures. The major advantage is the use of real-time fusion of two important imaging modalities. Whereas the use of CBCT is currently limited by static image guidance, TEE-XRF fusion guides the operator by image fusion of dynamic images. Furthermore, the technique offers a solution to the difficulties to interpret and superimpose the images of TEE alongside XRF in the mind of the implanting cardiologist.

Various reports on interventions involving TSP show integration of TEE-XRF in the workflow, resulting in a significant decrease in radiation exposure and fluoroscopy time when guided by Philips' EchoNavigator. Comparable results are shown in other cardiac interventions, in left atrial appendage occlusion up to 52% of total radiation exposure was reduced.<sup>42</sup> Only a trend in decrease of radiation and contrast exposure was observed in MitraClip procedures while, especially in more complex interventions, a larger benefit could be expected.<sup>42</sup> Therefore an interesting observed effect is that the higher the number of MitraClips placed, the shorter the time duration per clip when using Philips' EchoNavigator. Considering the higher number of clips that are necessary is related to a more complex procedure, the aforementioned observed effect emphasizes the importance of adequate 3D imaging.

### **Operator experience in HI solutions**

It can be argued that the beneficial effects when using HI during interventions are less pronounced in experienced teams. The software techniques discussed in this review aim to improve the current clinical workflow, procedural outcomes, and potentially clinical outcomes. Hybrid fusion imaging technologies such as Aortic Valve Guide, automate and standardize the segmentation process and identification of aortic cusps as well as perpendicular valve view. Therefore, upon sufficient image quality, these steps do not have to be performed by the operator, limiting intra- and interobserver variability, potentially providing more reliable procedural outcomes. Siemens' Aortic Valve Guide has shown to

significantly more likely provide excellent TAVI implant angles compared to CBCT or XRF alone, independent of operator experience.<sup>22</sup> Several reports described that the learning curve of TEE-XRF fusion caused an underestimation of the potential beneficial effect. Potentially a larger beneficial effect can be expected when more experience with TEE-XRF is gained.<sup>29,30</sup> Quantification of the effect of operator experience, however, requires studies with larger cohorts.

### **Institutional costs**

All major XRF vendors offer flat-panel detector systems that provide CBCT imaging options as well as pre-procedural image integration (Table 1), and market penetration is likely to increase in the future.<sup>9</sup> The institutional costs for these systems range between US\$1.2 million and US\$5.0 million depending on the vendor, specifications, single or biplane system, and the integration of various advanced imaging modalities such as 3D echocardiography for TEE-XRF fusion.<sup>43</sup> These prices can differ depending on the agreements made between the institution and vendor.

In theory, each XRF system can perform CBCT/3DRA acquisitions independent of the detector size. Larger XRF detectors should be preferred considering more information is acquired during a CBCT acquisition. This is important especially in case a 3D/3D registration with pre-procedural imaging without the need for fiducial markers is required. Moreover, lower costs per examination have been reported in favor of CBCT compared to XRF alone.<sup>44</sup> This can save procedural and healthcare costs.

### **Other cardiac applications**

While the focus in this review is on image-guided SHD and CHD procedures, cardiac interventions involving substrate targeting (e.g. endomyocardial biopsies, regenerative therapy) and/or modification (e.g. electrophysiology, cardiac resynchronization therapy [CRT] device implantations) could also benefit from interventional planning and image guidance provided by HI (see Figure 4).<sup>45,46</sup> However, this was considered to be outside the scope of the present paper.

### **Future developments**

Current fusion imaging software does not provide for motion compensation, specifically cardiac motion. A promising development is 4DRA, which can provide functional assessment of ventricular, valvular and vascular structures. These developments include optimizations of the current cone-beam back projection algorithms to acquire 4D reconstructions that include motion estimation and temporal parameterization by acquisition time.<sup>47-49</sup> Combinations of 4DRA with quick post-processing to generate 4D reconstructions opens the way for live dynamic 3D roadmaps which could potentially further increase interventional accuracy.

Another interesting HI development are augmented reality (AR)-based headsets. AR-based headsets enable projection of multidimensional full-color holograms superimposed on the real world using holographic lenses. An advanced sensor



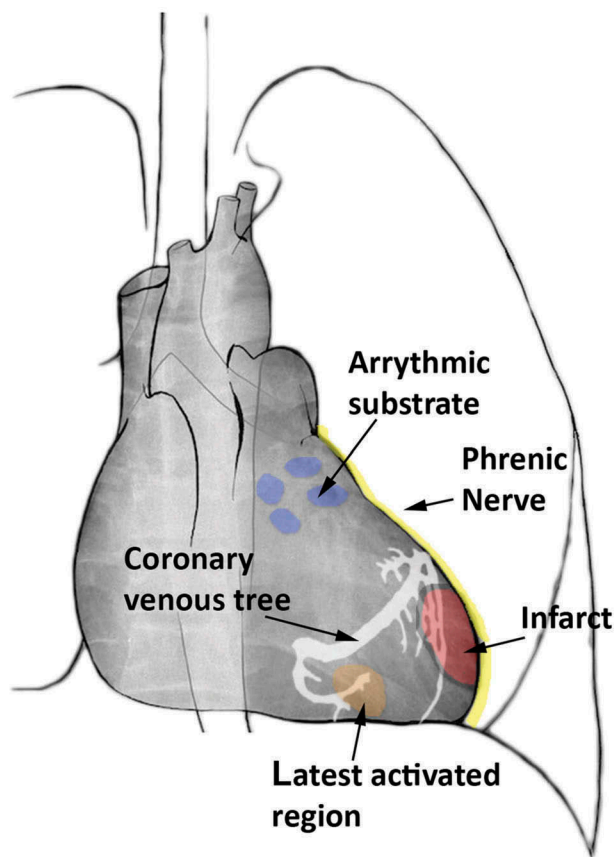


**Figure 4.** Schematic overview of potential 3D overlay markings onto XRF to guide cardiac resynchronization therapy (CRT) and electrophysiology cardiac interventions. The blue markings show targets for pulmonary vein isolation. In yellow the phrenic nerve is depicted, passing along the epicardium of the left ventricle. In red an infarcted region is visualized with corresponding border zone marked in black. The orange region is showing the latest activated area along with the coronary venous tree depicted in white.

system maps the environment around the user to anchor the holograms to the real world. Using voice commands and hand gestures AR-based headsets are very suitable to be introduced into the catheterization theatre. Potentially providing the cardiologist with additional 3D anatomical information and direct guidance projected on the patient.<sup>50</sup> Besides HI, there is an increased use of 3D printing of cardiac structures for pre-procedural interventional treatment planning.<sup>51</sup>

### Limitations

Although the available tools are comprehensive, the literature on the clinical use of the reviewed HI software solutions using XRF systems for cardiac procedures is still limited. Currently available studies are limited by small cohorts and focus on short-term procedural outcomes. Large multicenter studies are necessary to fully evaluate the current technologies and determine the long-term clinical benefits. Nevertheless, this review provides an overview of the tools that are clinically most used in SHD and CHD procedures and provides insight into the future directions for HI.

### Conclusion

Major interventional X-ray vendors offer HI software solutions which are safe and can aid the planning and image guidance of cardiovascular interventions. HI integration in SHD and CHD procedures has shown significant decreases in radiation and contrast exposure and complication rate. For visualization of more complex soft tissue characteristics, e.g. needed during cardiac resynchronization therapy device implantations, developments are ongoing and will provide standardized solutions in the future. Even though current HI technologies have limitations, HI provides support in the increasingly complex cardiac interventional procedures to provide better patient care.

### Funding

The research is part of the smartcare project funded by the TTI transition grant via the government and Top Sector Life Sciences & Health.

### ORCID

Hans Thijs van den Broek  <http://orcid.org/0000-0001-5680-5957>

### Disclosure statement

No potential conflicts of interest were reported by the authors.

### References

- Holmes DR, Mack MJ, Kaul S, et al. ACCF/AATS/SCAI/STS expert consensus document on transcatheter aortic valve replacement. *J Am Coll Cardiol.* 2012;59(13):1200–1254. doi:10.1016/j.jacc.2012.01.001.
- Ooi YK, Kelleman M, Ehrlich A, et al. Transcatheter versus surgical closure of atrial septal defects in children a value comparison. *JACC Cardiovasc Interv.* 2016;9(1):79–86. doi:10.1016/j.jcin.2015.09.028.
- Hijazi ZM, Awad SM. Pediatric cardiac interventions. *JACC Cardiovasc Interv.* 2008;1(6):603–611. doi:10.1016/j.jcin.2008.07.007.
- Takagi H, Ando T, Umemoto T. A review of comparative studies of MitraClip versus surgical repair for mitral regurgitation. *Int J Cardiol.* 2017;228(June 2016):289–294. doi:10.1016/j.ijcard.2016.11.153.
- Pantos I, Patatoukas G, Katritsis DG, Efsthathopoulos E. Patient radiation doses in interventional cardiology procedures. *Curr Cardiol Rev.* 2009;5(1):1–11. doi:10.2174/157340309787048059.
- Voskuil M, Sievert H, Arslan F. Guidance of interventions in structural heart disease; three-dimensional techniques are here to stay. *Neth Heart J.* 2017;25(2):63–64. doi:10.1007/s12471-016-0945-0.
- Cavalcante JL, Lalude OO, Schoenhagen P, Lerakis S. Cardiovascular magnetic resonance imaging for structural and valvular heart disease interventions. *JACC Cardiovasc Interv.* 2016;9(5):399–425. doi:10.1016/j.jcin.2015.11.031.
- Thaden JJ, Sanon S, Geske JB, et al. Echocardiographic and fluoroscopic fusion imaging for procedural guidance: an overview and early clinical experience. *J Am Soc Echocardiogr.* 2016;29(6):503–512. doi:10.1016/j.echo.2016.01.013.
- Schwartz JG, Neubauer AM, Fagan TE, et al. Potential role of three-dimensional rotational angiography and C-arm CT for valvular repair and implantation. *Int J Cardiovasc Imaging.* 2011;27(8):1205–1222. doi:10.1007/s10554-011-9839-9.
- Numburi UD, Kapadia SR, Schoenhagen P, et al. Optimization of acquisition and contrast injection protocol for C-arm CT imaging in transcatheter aortic valve implantation: initial experience in a



- swine model. *Int J Cardiovasc Imaging*. 2013;29(2):405–415. doi:10.1007/s10554-012-0075-8.
11. Balzer JC, Boering YC, Mollus S, et al. Left ventricular contrast injection with rotational C-arm CT improves accuracy of aortic annulus measurement during cardiac catheterisation. *EuroIntervention*. 2014;10(3):347–354. doi:10.4244/EIJV1013A60.
  12. Peters M, Krings G, Koster M, et al. Effective radiation dosage of three-dimensional rotational angiography in children. *Europace*. 2014;17(4):611–616. doi:10.1093/europace/euu207.
  13. Haddad L, Waller BR, Johnson J, et al. Radiation protocol for three-dimensional rotational angiography to limit procedural radiation exposure in the pediatric cardiac catheterization lab. *Congenit Heart Dis*. 2016;11:637–646. doi:10.1111/chd.12356.
  14. De Buck S, Alzand BSN, Wielandts JY, et al. Cardiac three-dimensional rotational angiography can be performed with low radiation dose while preserving image quality. *Europace*. 2013;15(12):1718–1724. doi:10.1093/europace/eut140.
  15. Starek Z, Lehar F, Jez J, et al. Periprocedural 3D imaging of the left atrium and esophagus: comparison of different protocols of 3D rotational angiography of the left atrium and esophagus in group of 547 consecutive patients undergoing catheter ablation of the complex atrial arrhythmias. *Int J Cardiovasc Imaging*. 2016;1–9. doi:10.1007/s10554-016-0888-y.
  16. Eloit L, Bacher K, Steenbeke F, et al. Three-dimensional rotational X-ray acquisition technique is reducing patients' cancer risk in coronary angiography. *Catheter Cardiovasc Interv*. 2013;82(4):419–427. doi:10.1002/ccd.24879.
  17. Picano E, Vañó E, Rehani MM, et al. The appropriate and justified use of medical radiation in cardiovascular imaging: a position document of the ESC Associations of Cardiovascular Imaging, Percutaneous Cardiovascular Interventions and Electrophysiology. *Eur Heart J*. 2014;35(10):665–672. doi:10.1093/eurheartj/ehu394.
  18. Glatz AC, Zhu X, Gillespie MJ, Hanna BD, Rome JJ. Use of angiographic CT imaging in the cardiac catheterization laboratory for congenital heart disease. *JACC Cardiovasc Imaging*. 2010;3(11):1149–1157. doi:10.1016/j.jcmg.2010.09.011.
  19. Sinning J-M, Ghanem A, Steinhäuser H, et al. Renal function as predictor of mortality in patients after percutaneous transcatheter aortic valve implantation. *JACC Cardiovasc Interv*. 2010;3(11):1141–1149. doi:10.1016/j.jcin.2010.09.009.
  20. Jabbour A, Ismail TF, Moat N, et al. Multimodality imaging in transcatheter aortic valve implantation and post-procedural aortic regurgitation: comparison among cardiovascular magnetic resonance, cardiac computed tomography, and echocardiography. *J Am Coll Cardiol*. 2011;58(21):2165–2173. doi:10.1016/j.jacc.2011.09.010.
  21. Singh GD, Smith TW, Rogers JH. Targeted transseptal access for MitraClip percutaneous mitral valve repair. *Interv Cardiol Clin*. 2017;5(1):55–69. doi:10.1016/j.iccl.2015.08.005.
  22. Poon KK, Crowhurst J, James C, et al. Impact of optimising fluoroscopic implant angles on paravalvular regurgitation in transcatheter aortic valve replacements – Utility of three-dimensional rotational angiography. *EuroIntervention*. 2012;8(5):538–545. doi:10.4244/EIJV8I5A84.
  23. Binder RK, Leipsic J, Wood D, et al. Prediction of optimal deployment projection for transcatheter aortic valve replacement: angiographic 3-dimensional reconstruction of the aortic root versus multidetector computed tomography. *Circ Cardiovasc Interv*. 2012;5(2):247–252. doi:10.1161/CIRCINTERVENTIONS.111.966531.
  24. Samim M, Stella PR, Agostoni P, et al. Automated 3D analysis of pre-procedural MDCT to predict annulus plane angulation and C-arm positioning: benefit on procedural outcome in patients referred for TAVR. *JACC Cardiovasc Imaging*. 2013;6(2):238–248. doi:10.1016/j.jcmg.2012.12.004.
  25. Van Linden A, Kempfert J, Blumenstein J, et al. Manual versus automatic detection of aortic annulus plane in a computed tomography scan for transcatheter aortic valve implantation screening. *Eur J Cardio-Thoracic Surg*. 2014;46(2):207–212. doi:10.1093/ejcts/ezt600.
  26. Vaitkus PT, Wang DD, Greenbaum A, Guerrero M, O'Neill W. Assessment of a novel software tool in the selection of aortic valve prosthesis size for transcatheter aortic valve replacement. *J Invasive Cardiol*. 2014;26:328–332.
  27. Kliger C, Jelnin V, Sharma S, et al. CT angiography-fluoroscopy fusion imaging for percutaneous transapical access. *JACC Cardiovasc Imaging*. 2014;7(2):169–177. doi:10.1016/j.jcmg.2013.10.009.
  28. Blanke P, Dvir D, Naoum C, et al. Prediction of fluoroscopic angulation and coronary sinus location by CT in the context of transcatheter mitral valve implantation. *J Cardiovasc Comput Tomogr*. 2015;9(3):183–192. doi:10.1016/j.jcct.2015.02.007.
  29. Jone P-N, Ross MM, Bracken JA, et al. Feasibility and safety of using a fused echocardiography/fluoroscopy imaging system in patients with congenital heart disease. *J Am Soc Echocardiogr*. 2016;29(6):513–521. doi:10.1016/j.echo.2016.03.014.
  30. Sündermann SH, Biaggi P, Grünenfelder J, et al. Safety and feasibility of novel technology fusing echocardiography and fluoroscopy images during MitraClip interventions. *EuroIntervention*. 2014;9(10):1210–1216. doi:10.4244/EIJV9I10A203.
  31. Quaife RA, Salcedo EE, Carroll JD. Procedural guidance using advance imaging techniques for percutaneous edge-to-edge mitral valve repair. *Curr Cardiol Rep*. 2014;16(2):452. doi:10.1007/s11886-013-0452-5.
  32. Goreczny S, Moszura T, Dryzek P, et al. Three-dimensional image fusion guidance of percutaneous pulmonary valve implantation to reduce radiation exposure and contrast dose: a comparison with traditional two-dimensional and three-dimensional rotational angiographic guidance. *Neth Heart J*. 2017;25(2):91–99. doi:10.1007/s12471-016-0941-4.
  33. Nguyen HH, Balzer DT, Murphy JJ, Nicolas R, Shahanavaz S. Radiation exposure by three-dimensional rotational angiography (3DRA) during trans-catheter melody pulmonary valve procedures (TMPV) in a pediatric cardiac catheterization laboratory. *Pediatr Cardiol*. 2016;37(8):1429–1435. doi:10.1007/s00246-016-1453-0.
  34. Faletra FF, Biasco L, Pedrazzini G, et al. Echocardiographic-fluoroscopic fusion imaging in transseptal puncture: a new technology for an old procedure. *J Am Soc Echocardiogr*. 2017;30(9):886–895. doi:10.1016/j.echo.2017.05.001.
  35. Afzal S, Veulemans V, Balzer J, et al. Safety and efficacy of transseptal puncture guided by real-time fusion of echocardiography and fluoroscopy. *Neth Heart J*. 2017;25(2):131–136. doi:10.1007/s12471-016-0937-0.
  36. Berman DP, Khan DM, Gutierrez Y, Zahn EM. The use of three-dimensional rotational angiography to assess the pulmonary circulation following cavo-pulmonary connection in patients with single ventricle. *Catheter Cardiovasc Interv*. 2012;80(6):922–930. doi:10.1002/ccd.23461.
  37. Starman NLP, Krings GJ, Molenschot MMC, van der Stelt F, Breur JMPJ. Three-dimensional rotational angiography in children with an aortic coarctation. *Neth Heart J*. 2016;24:666–674. doi:10.1007/s12471-016-0899-2.
  38. Stenger A, Dittrich S, Glöckler M. Three-dimensional rotational angiography in the pediatric Cath lab: optimizing aortic interventions. *Pediatr Cardiol*. 2016;37(3):528–536. doi:10.1007/s00246-015-1310-6.
  39. Goreczny S, Dryzek P, Morgan GJ, et al. Novel three-dimensional image fusion software to facilitate guidance of complex cardiac catheterization 3D image fusion for interventions in CHD. *Pediatr Cardiol*. 2017;38(6):1133–1142. doi:10.1007/s00246-017-1627-4.
  40. Suntharos P, Setser RM, Bradley-Skelton S, Prieto LR. Real-time three dimensional CT and MRI to guide interventions for congenital heart disease and acquired pulmonary vein stenosis. *Int J Cardiovasc Imaging*. 2017;33(10):1619–1626. doi:10.1007/s10554-017-1151-x.
  41. Noseworthy PA, Malchano ZJ, Ahmed J, et al. The impact of respiration on left atrial and pulmonary venous anatomy: implications for image-guided intervention. *Heart Rhythm*. 2005;2(11):1173–1178. doi:10.1016/j.hrthm.2005.08.008.
  42. Jungen C, Zeus T, Balzer J, et al. Left atrial appendage closure guided by integrated echocardiography and fluoroscopy imaging



- reduces radiation exposure. *PLoS One*. 2015;10(10):1–13. doi:10.1371/journal.pone.0140386.
43. Kpodonu J. Hybrid cardiovascular suite: the operating room of the future. *J Card Surg*. 2010;25(6):704–709. doi:10.1111/j.1540-8191.2010.01111.x.
  44. Kriatselis C, Nedios S, Akrivakis S, et al. Intraprocedural imaging of left atrium and pulmonary veins: a comparison study between rotational angiography and cardiac computed tomography. *PACE - Pacing Clin Electrophysiol*. 2011;34(3):315–322. doi:10.1111/j.1540-8159.2010.02969.x.
  45. Rogers T, Ratnayaka K, Karmarkar P, et al. Real-time magnetic resonance imaging guidance improves the diagnostic yield of endomyocardial biopsy. *JACC Basic to Transl Sci*. 2016;1(5):376–383. doi:10.1016/j.jacbts.2016.05.007.
  46. Behar JM, Rajani R, Rinaldi CA. Guided left ventricular lead placement for cardiac resynchronization therapy: an opportunity for image integration. *Eur J Heart Fail*. 2017;19(3):435–436. doi:10.1002/ejhf.716.
  47. Mory C, Auvray V, Zhang B, et al. Cardiac C-arm computed tomography using a 3D + time ROI reconstruction method with spatial and temporal regularization. *Med Phys*. 2014;41(2):21903. doi:10.1118/1.4860215.
  48. Wielandts J-Y, De Buck S, Michielsens K, et al. Multi-phase rotational angiography of the left ventricle to assist ablations: feasibility and accuracy of novel imaging. *Eur Hear J - Cardiovasc Imaging*. 2016;17(2):162–168. doi:10.1093/ehjci/jev120.
  49. Taubmann O, Haase V, Lauritsch G, et al. Assessing cardiac function from total-variation-regularized 4D C-arm CT in the presence of angular undersampling. *Phys Med Biol*. 2017;62(7):2762–2777. doi:10.1088/1361-6560/aa6241.
  50. Kuhlemann I, Kleemann M, Jauer P, Schweikard A, Ernst F. Towards X-ray free endovascular interventions – using HoloLens for on-line holographic visualisation. *Healthc Technol Lett*. 2017;4:184–187. doi:10.1049/htl.2017.0061.
  51. Meier LM, Meineri M, Qua Hiansen J, Horlick EM. Structural and congenital heart disease interventions: the role of three-dimensional printing. *Neth Heart J*. 2017;25(2):65–75. doi:10.1007/s12471-016-0942-3.